figuration due to a greater chiral selectivity. The enantiomeric dansyl amino acids, which have intramolecular hydrophobic interaction of the relatively long side chains with the dansyl group, can attack copper (II) chelate to form a ternary complex by SN2 reaction. L-Forms of DNS-amino acids are able to produce both cis and trans configuration due to the steric effect. Therefore, most of D-DNS-amino acids are less retained than L-DNS-amino acids except Phe, Tyr, and Asn. The dansylated phenylalanine and tyrosine whose ternary complexes seem to have a greater hydrophobic interaction in cis product showed the reverse elution order because the proline ring of the chelate has the same plane with the naphthyl ring of the dansylated amino acids. The dansylated asparagine containing the basic alkyl group also showed elution of L-form ahead of D-form because of the hydrophilicity of the side chain.

Acknowledgement. Financial support from the Korea Science and Engineering Foundation is gratefully acknowledged.

Reference

1. E. Gil-Av and S. Weinstein, *CRC Handbook*, **1**, 429 (1984).
2. S. H. Lee, J. Y. Ryu, and K. S. Park, *Bull. Korean Chem. Soc.*, **7**, 45 (1986).
3. S. H. Lee, T. S. Oh, and K. S. Park, *J. Korean Chem. Soc.*, **20**, 216 (1986).
4. S. Lam, and G. Milikin, *J. Chromatogr.*, **368**, 413 (1986).
5. S. Lam, *J. Chromatogr.*, **335**, 157 (1986).
6. T. Takeuchi, H. Asai, Y. Hashimoto, K. Watanabe, and D. Ishii, *J. Chromatogr.*, **331**, 99 (1985).
7. R. Wernicke, *J. Chromatogr. Sci.*, **23**, 39 (1985).
8. M. H. Engel and S. A. Macko, *Anal. Chem.*, **56**, 2598 (1984).
9. N. Nimura, A. Toyama, and T. Kinoshita, *J. Chromatogr.*, **316**, 547 (1984).
10. S. Iam, and A. Karmen, *J. Chromatogr.*, **289**, 339 (1984).
11. E. Grushika, R. Ieshem, and C. Gilon, *J. Chromatogr.*, **255**, 41 (1983).
12. N. Nimura, T. Suzuki, Y. Kasahara, and T. Kinoshita, *Anal. Chem.*, **53**, 1380 (1981).
13. I. D. Hay, T. M. Annesley, N. S. Jiang, and C. A. Gorman, *J. Chromatogr.*, **226**, 383 (1981).
14. Y. Tapuhi, N. Miller, and B. I. Karger, *J. Chromatogr.*, **205**, 325 (1981).
15. S. H. Lee, D. S. Oh, and B. E. Kim, *Bull. Korean Chem. Soc.*, **9**, 341 (1988).
16. P. E. Hara and E. Gil-Av, *Science*, **204**, 1226 (1976).
17. E. Gil-Av, A. Tishibee, and P. E. Hara, *J. Am. Chem. Soc.*, **102**, 5115 (1980).
18. E. Oelrich, H. Preusch, and E. Wilhelm, *HRR and CC*, **3**, 269 (1980).
19. S. Lam, F. Chow and A. Karmen, *J. Chromatogr.*, **199**, 295 (1980).

Ionic Conductivity by A Complex Admittance Method

Chy Hyung Kim* and Eung Dong Kim

Department of Chemistry and Electronic Engineering, Chongju University, Chongju 360-764.* *Received June 3, 1989*

The ionic conductivity of polycrystalline, glass, and glass-ceramic silicates was measured using two-terminal AC method with blocking electrode over a frequency range of 100 Hz to 100 KHz in the temperature range of 200 °C to 320 °C. Analysing the capacitance (C), susceptance (B), impedance(Z), and conductance (G) under the given conditions, an equivalent circuit containing temperature and frequency dependent component is proposed. Higher capacitance could be observed in the low frequency region and on the improved ionic migration conditions *i.e.*, at higher temperature in a better ionic conductor. Also the electrode polarization built up at the electrode-specimen interface could be sorted out above 10 KHz. However, grain boundary contribution couldn't be extracted from the bulk resistance over the frequency range measured here.

Introduction

The conductivity measurement by AC method in solid electrolytes has advantages since interfacial polarization between the electrode-electrolyte and the grain boundary effects can be sorted out at the proper frequencies. While the electrode polarization can be eliminated by using reversible electrode there are still other problems to find the proper electrode material when there is more than one type of mobile ion and to handle the electrode in molten state.

More complete model using AC measurement is the complex admittance method applied by Bauerle[1]. This method has been used by many scientists for various solid electrolytes[2]. The complex method is originally from Cole and Cole complex permittivity diagrams[3].

The complex admittance (Y) can be expressed as the sum of the coductance (G) and the susceptance (B).

$$Y = G + iB$$

From the plot of susceptance *vs.* conductance, the resistance

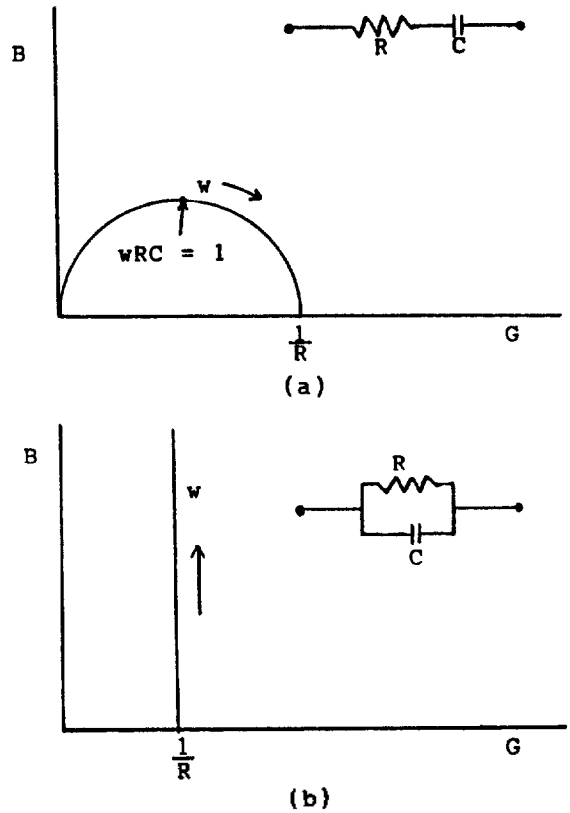

Figure 1. Admittance plots for simple *R-C* circuit.

value can be derived from the circular arc intercept on the *G*-axis and the capacitance value from the expression involving the frequency at the peak of the circular arc (Figure 1). When the admittance plot gives a circular arc a series *R-C* circuit is dominant (Figure 1(a)), whereas a straight line indicates more characteristic parallel *R-C* circuit (Figure 1(b)).

The specimens investigated in this experiment are $M_3RESi_3O_9$ (M = Li or Na, RE = Sm, Y, or Gd)[4,5] and $Na_5SmSi_4O_{12}$[6] type materials which are known to have $[Si_6O_{18}]$ and $[Si_{12}O_{36}]$ rings.

Especially, $Na_5RESi_4O_{12}$ (RE = rare earth) is the one of the best ionic conductors due to the one dimensional open pathway of Na^+ ion in its structure. $Na_3RESi_3O_9$ structure has vacant holes which can accept more Na^+ ions to improve the conductivity[7,8]. The glass and glass-ceramic silicate compounds have also been studied[9].

In this paper we discuss the resistance and capacitance factors in Li^+ or Na^+ ion conducting materials, and show how these systems can be described as an equivalent circuit by utilizing the *AC* complex method. This attempt will be meaningful to know the relations between intrinsic factors influencing the conductivity, and to sort out them by selecting the proper frequencies. No a priori assumption is necessary on the equivalent circuit of the cell.

Experimental

General solid state preparative method was used to synthesize the samples[5,6,9]. To prepare $Na_{3.2}Sm_{0.7}Si_{2.9}P_{0.1}O_{8.7}$ starting materials Na_2CO_3, SiO_2, Sm_2O_3, and $NH_4H_2PO_4$ were mixed in proper molar ratios and fired overnight in a covered platinum crucible at 895 °C.

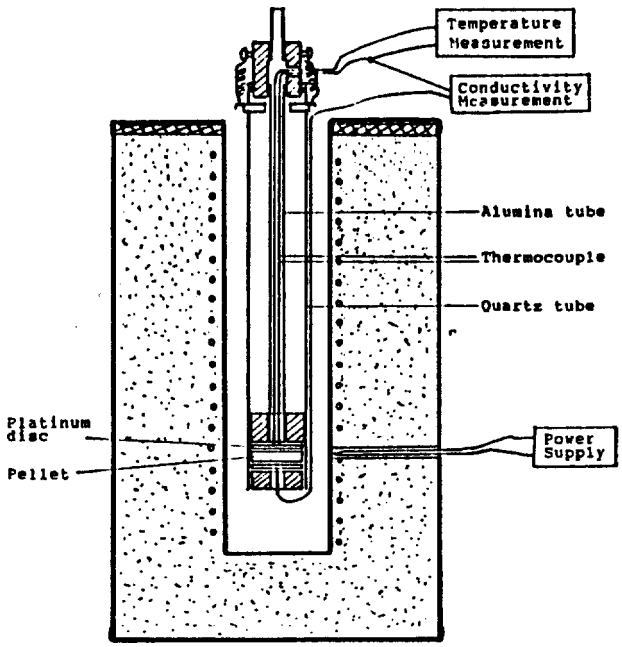

Figure 2. Sample holder for conductivity measurement.

For the specimen $Li_{3.2}Gd_{0.7}Si_{2.9}P_{0.1}O_{8.7}$ powders of $Na_{3.2}Gd_{0.7}Si_{2.9}P_{0.1}O_{8.7}$ were treated with excess molten $LiNO_3$ at 350 °C and washed with distilled water, filtered, and dried at 150 °C. Glasses $Na_3YSi_3O_9$ and $Na_5SmSi_4O_{12}$ could be obtained by fusing the starting materials at 1250 °C and at 1350 °C, pouring the molten materials quickly into a stainless steel mold before they were solidified. For the production of glass-ceramic $Na_5SmSi_4O_{12}$ the glass $Na_5SmSi_4O_{12}$ was placed on a graphite plate to prevent adhesion at high temperature, heated at 845 °C and then annealed.

Pellets for the conductivity measurement were prepared as described in the references[5,9]. 2000 Å thick of gold layer was deposited as blocking electrode and a thin layer of chromium (~400 Å) was intercalated between the surface of the pellet and gold layer for strong adhesion. Two-terminal *AC* measurement was performed over the range 10^2-10^5 Hz especially, eleven frequencies (100, 120, 200, 400, 1K, 2K, 4K, 10K, 20K, 40K, and 100K Hz) were selected at 1 volt using a Hewlett-Packard 4274A Multi-Frequency LCR meter. Figure 2 shows the schematic drawing of the sample holder used for the measurement. Once the sample is introduced into the furnace a dry nitrogen gas is flowed to prevent the chromium layer on the sample from oxidizing to Cr_2O_3, which could act as an electric insulator.

Results and Discussion

$Na_{3.2}Sm_{0.7}Si_{2.9}P_{0.1}O_{8.7}$. Figure 3 shows the capacitances of samarium silicate at four temperatures depending on the frequency. Higher capacitance can be observed at low frequency and at high temperature. In the very high frequency region capacitance *vs.* log ω curve gives a constant value ($C_{ind.}$) which is intrinsic and independent on the temperature and frequency. The approximate value of $C_{ind.}$ was taken from the capacitance at 100 KHz. The shape of the curve suggests that the relation between log $(C-C_{ind.})$ and log ω may be expressed linearly as can be seen in Figure 4.

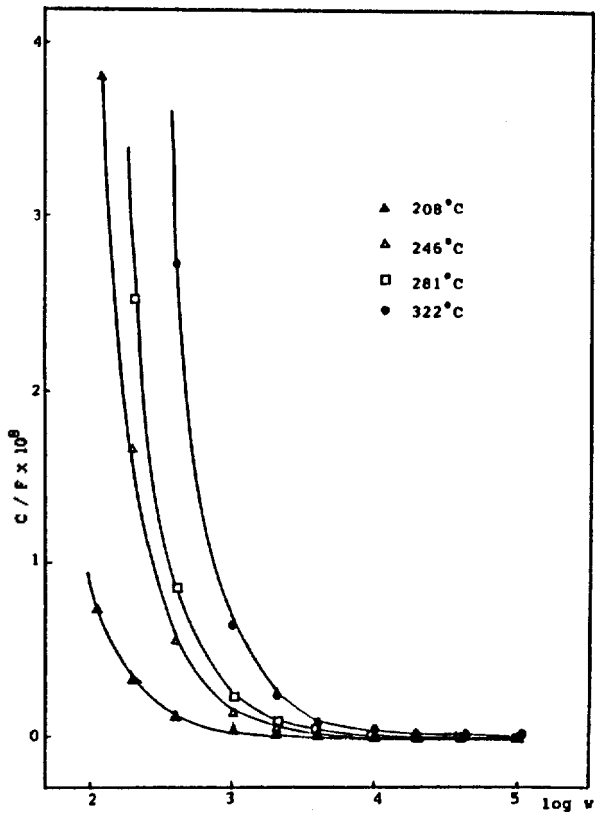

Figure 3. Capacitance *vs.* log ω for samarium silicate at four temperatures.

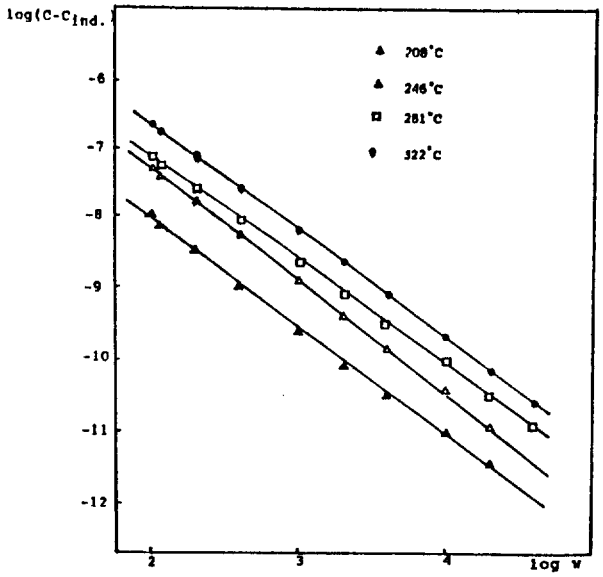

Figure 4. log $(C - C_{ind})$ *vs.* log ω for samarium silicate at four temperatures.

$$\log(C-C_{ind})=\log a+b\log\omega$$

where log a is the intercept and b is the slope. Thus

$$C=C_{ind}+a\omega^{b}$$

The values of a and b in Table 1 were estimated by least square method. The magnitude of each a and b value does not have any special meaning except they are determined from the experimental data.

Table 1. Parameters for $Na_{3.2}Sm_{0.7}Si_{2.9}P_{0.1}O_{8.7}$

t(°C)	slope (b)	intercept (log a)	a	$C(F)$ at 100 KHz
208	-1.46	-5.14	7.18×10^{-6}	2.8×10^{-11}
246	-1.59	-4.11	7.80×10^{-5}	4.6×10^{-11}
281	-1.45	-4.26	5.47×10^{-5}	2.4×10^{-11}
322	-1.53	-3.59	2.59×10^{-4}	11.8×10^{-11}

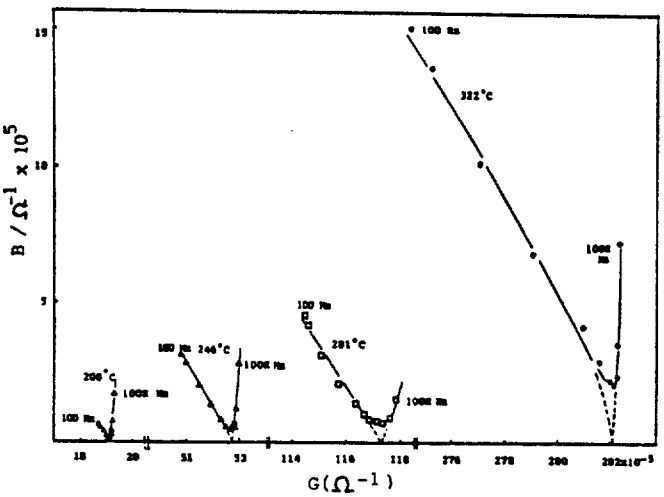

Figure 5. Complex admittance plots for samarium silicate at four temperatures.

Table 2. Parameters for $Na_{3.2}Sm_{0.7}Si_{2.9}P_{0.1}O_{8.7}$

t(°C)	slope (B)	intercept (log A)	A
208	0.39	-7.70	2.02×10^{-8}
246	0.56	-8.56	2.74×10^{-9}
281	×	×	×
322	×	×	×

Figure 5 shows the B–G plots of samarium silicate. The relation between log $(G-\frac{1}{R_B})$ and log w can also be written as

$$\log(G-\frac{1}{R_B})=\log A+B\log\omega$$

then $G=\frac{1}{R_B}+A\omega^{B}$

where R_B is the resistance of polycrystalline, in other words, the resistance of grain (R_g) plus resistance of grain boundary (R_{gb}). The values of A and B at low temperature are listed in Table 2. At high temperature, most G values are less than $1/R_B$.

As can be seen in Figure 5, parallel R–C circuit is dominant at high frequency and at low temperature. So, admittance for those conditions is

$$Y=G+j\omega C=\frac{1}{R_B}+A\omega^{B}+j(\omega C_{ind}+a\omega^{b+1})$$

If $Y^*=A\omega^{B}+ja\omega^{b+1}$ where Y^* is a frequency dependent component, the equivalent circuit can be drawn as in Figure 6.

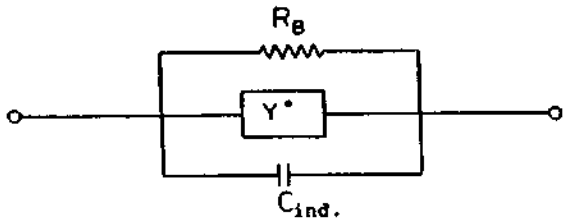

Figure 6. Equivalent circuit model at low temperature, high frequency.

Table 3. Parameters for $Na_{3.2}Sm_{0.7}Si_{2.9}P_{0.1}O_{8.7}$

t(°C)	slope (n)	intercept (log m)	m
208	-0.57	3.15	1.40×10^3
246	-0.68	3.19	1.55×10^3
281	-0.42	2.12	1.30×10^2
322	-0.67	2.28	1.90×10^2

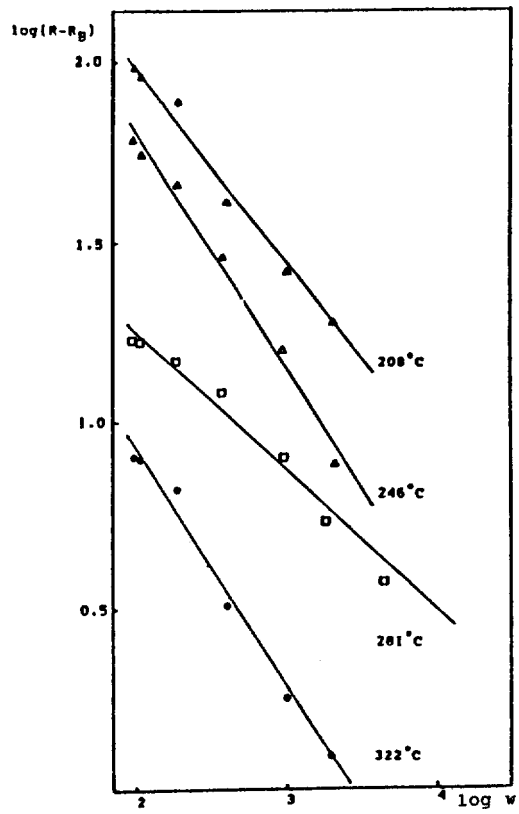

Figure 7. log $(R-R_B)$ *vs.* log ω for samarium silicate at four temperatures.

At low frequency and high temperature the B-G plot shows the characters of series R-C circuit (Figure 5). In this case the occurrence of circular arc in B-G plot is equivalent to a straight line in the $X-R$ plot. So $-X/(R-R_B)$ indicates the slope(k) of the line. Figure 7 gives the plot of log $(R-R_B)$ against log w. We can write

$$\log(R-R_B)=\log m+n\log\omega$$

$$R-R_B=m\omega^n$$

Values of n, m are evaluated in Table 3. Impedance at the

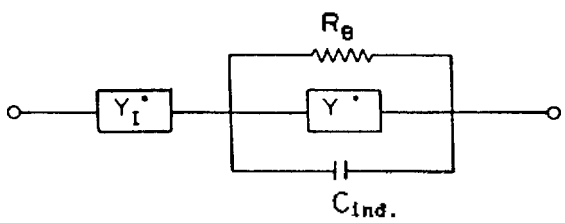

Figure 8. Equivalent circuit model at full experimental range.

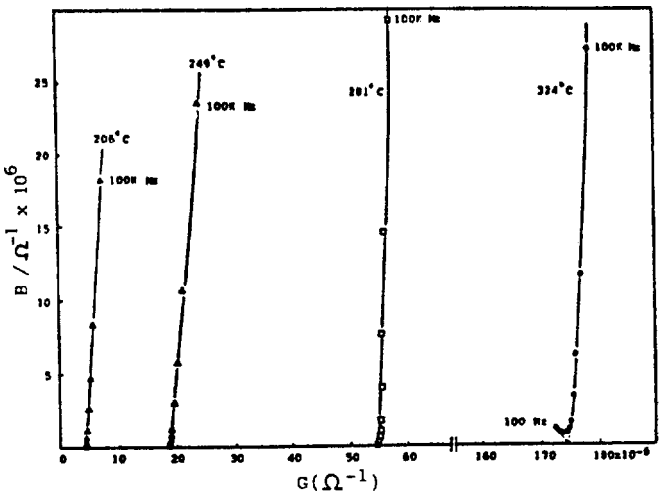

Figure 9. Complex admittance plots for gadolinium silicate at four temperatures.

low frequency (high temperature) is represented as

$$Z_I=R+jX$$

$$=R_B+m\omega^n-jk(R-R_B)$$

Hence the frequency dependent impedance part

$$Z_I^*=m\omega^n-jkm\omega^n$$

$$=m\omega^n-jm'\omega^n \quad \text{where } km=m'$$

then

$$Y_I^*=\frac{1}{Z_I^*}=\frac{m\omega^{-n}}{m^2+m'^2}+j\frac{m'\omega^{-n}}{m^2+m'^2}$$

It is possible to get a modified equivalent circuit model by introducing Y_I^* which belongs to a series part (Figure 8). Y_I^* is associated mainly with the electrolyte-electrode interface. Thus when high frequency is applied to the sample at low temperature mobile ion in the structure cannot arrive at the interface so easily, where the effect of Y_I^* is diminished. This can also be confirmed by plotting the permittivity against the frequency[10].

$Li_{3.2}Gd_{0.7}Si_{2.9}P_{0.1}O_{8.7}$, glass $Na_5YSi_3O_9$, glass $Na_5SmSi_4O_{12}$, and glass-ceramic $Na_3SmSi_4O_{12}$. Although same experimental conditions are applied to the different materials different equivalent circuits can be expected. Of those four materials $Li_{3.2}Gd_{0.7}Si_{2.9}P_{0.1}O_{8.7}$ is the worst conductor and the equivalent R-C circuit is almost parallel (Figure 9). On the other hand, the contribution of the component of series R-C circuit is dominant in the highest ionic conductor glass-ceramic $Na_5SmSi_4O_{12}$ (Figure 10). In glasses $Na_3YSi_3O_9$ and $Na_5SmSi_4O_{12}$ similar characters discussed in

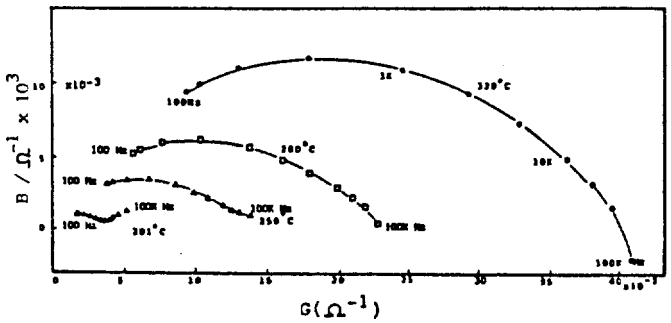

Figure 10. Complex admittance plots for glass-ceramic $Na_5SmSi_4O_{12}$ at four temperatures.

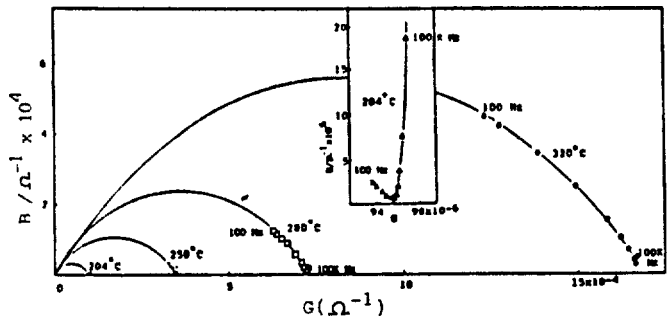

Figure 11. Complex admittance plots for glass $Na_3YSi_3O_9$ at four temperatures.

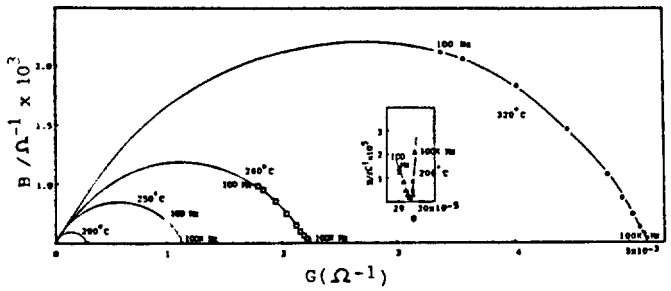

Figure 12. Complex admittance plots for glass $Na_5SmSi_4O_{12}$ at four temperatures.

$Na_{3.2}Sm_{0.7}Si_{2.9}P_{0.1}O_{8.7}$ are seen in Figures 11 and 12. Therefore it can be said that higher ionic migration conditions lead to the series R-C circuit character mainly due to easier formation of double layers at the electrolyte-electrode system and at the grain-grain boundary interface.

Usually higher capacitance can be observed at higher conducting materials (Figures 13 and 14), even though the degree of the increment of capacitance against the increment of temperature ($\Delta C/\Delta T$) is different depending on the cells. Figure 14 shows the Arrhenius plots of the ionic conductivity as a function of temperature. The conductivity was estimated from the value of R_B obtained in B-G plot, thickness, and the area of the pellet measured in this experiment. The separation of R_g and R_{gb} from the resistance of polycrystalline was impossible at the frequency range of 10^2–10^5 Hz except sorting out the electrode polarization effect in the high frequency range.

Acknowledgement. Parts of this work have been done in Dr. E. Banks' laboratory at Polytechnic University of New York. I appreciate him who helped me during stay there.

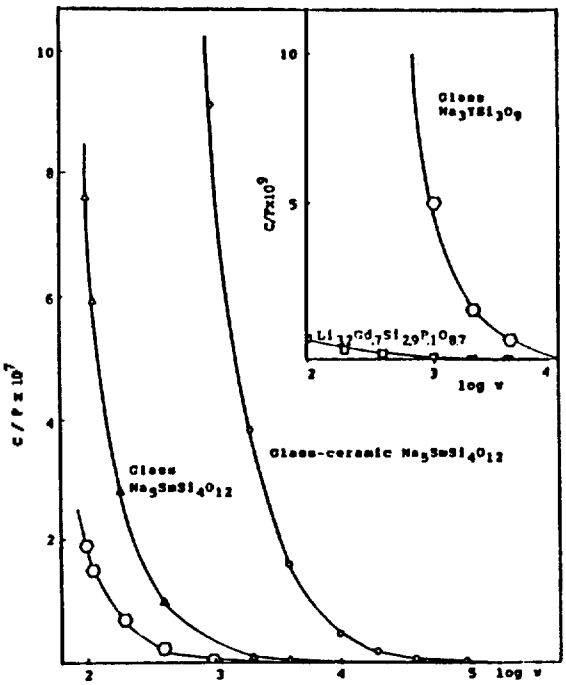

Figure 13. Capacitance *vs.* log w at 280 °C.

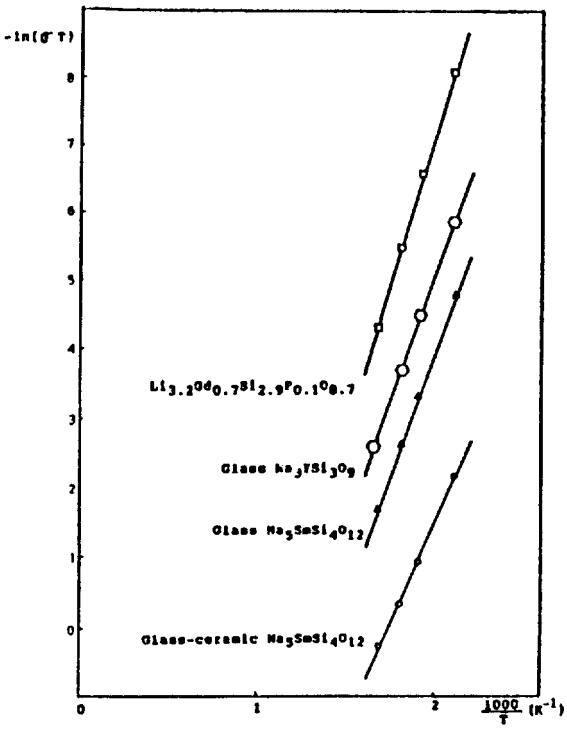

Figure 14. Arrhenius plots as a function of temperature.

References

1. J. E. Bauerle, *J. Phys. Chem. Solid*, **30**, 2657 (1969).
2. (a) E. Schouler, A. Hammou, and M. Kleitz, *Mater. Res. Bull.*, **11**, 1137 (1976); (b) A. Hammou, *J. Chim. Phys.*, **72**, 431 (1975); (c) A. Hammou and C. Deportes, *ibid.*, **71**, 1071 (1974); (d) N. M. Beekmans and L. Heyne, *Electrochim. Acta*, **21**, 303 (1976); (e) I. D. Raistrick, Chun Ho, and R. A. Huggins, *J. Electrochem. Soc.*, **123**, 1469

(1976); (f) P. G. Bruce and A. R. West, *J. Electrochem. Soc.*, **130**, 662 (1983).
3. K. S. Cole and R. H. Cole, *J. Chem. Phys.*, **9**, 341 (1941).
4. R. D. Shannon, T. E. Gier, C. M. Foris, J. A. Nelen, and D. E. Appleman, *Phys. Chem. Miner.*, **5**, 245 (1980).
5. C. H. Kim, B. Qiu, and E. Banks, *J. Electrochem. Soc.*, **132**, 1340 (1985).
6. R. D. Shannon, B. E. Tayler, T. E. Gier, H. Y. Chen, and T. Berzins, *Inorg. Chem.*, **17**, 958 (1978).
7. P. Mondal and J. W. Jeffery, *Acta Crystallogr.*, B **31**, 689 (1975).
8. C. H. Kim and E. Banks, *Bull. Kor. Chem. Soc.*, **8**, 6 (1987).
9. E. Banks and C. H. Kim, *J. Electrochem. Soc.*, **132**, 2617 (1985).
10. A. R. West, "Solid State Chemistry and Its Applications", p. 535, John Wiley & Sons, New York, 1984.

Studies of the Reactions between P-donors and [(exo-6-R-η^5-2-MeO-C_6H_5)$Mn(CO)_2NO$]PF_6

Taeg-Hwan Hyeon, Taek-Mo Chung, and Young Keun Chung*

Department of Chemistry, College of Natural Sciences, Seoul National University, Seoul 151-742
Received June 15, 1989

Synthetic studies have been carried out for the addition or substitution of phosphorus nucleophiles to the cation [(exo-6-R-η^5-2-MeO-C_6H_5)$Mn(CO)_2NO$]PF_6, **2**. PPh_3 reacts with **2** to yield the CO displaced product and $MePPh_2$ attacks the dienyl ring of **2** to yield the phosphonium adduct or the metal to give the CO displaced depending upon the reaction temperatures. Nucleophilic addition of $HPPh_2$ to the dienyl ring of **2** gives a neutral substituted product. $P(OMe)_3$ reacts with **2** to yield a mixture of ring adduct and CO displaced product at room temperature. At −20 °C, $P(OMe)_3$ attacks the dienyl ring of **2** to give a posphonium adduct, which underwent Arbuzov reaction. This reaction affords a new route to the phosphonate complexes.

Introduction

Tertiary phosphines and phosphites have been proved to be particulary convenient nucleophiles for mechanistic investigations because they generally undergo clean addition to the π-hydrocarbon ligands to yield stable phosphonium adducts[1]. Apart from their intrinsic interest, these phosphonium adducts are potential precursors for synthetically useful organometallic ylides. The phosphonium adducts have been used successfully in preparing new derivatives of (benzene) tricarbonylchromium[2], ferrocene[3], and six- and seven-membered ring dienyl complexes of $Fe(CO)_3$[4]. As part of a systematic study of the mechanism of nucleophilic attack on π-hydrocarbon ring ligands, Sweigart and Chung[5] reported the kinetic data for the addition of phosphorus and nitrogen donor to $[(C_6H_6R)Mn(CO)(NO)(L)]^+$ (R = Me, Ph; L = CO, PPh_3) complexes, **1**, to give cyclohexadiene complexes. The present paper reports further synthetic studies of the reaction of [(exo-6-R-η^5-2-$MeOC_6H_5$)$Mn(CO)_2NO$]$^+$ (R = Me, Ph, and $CH_2C(O)CH_3$), **2**, with phosphines $RPPh_2$ (R = H, Me, and Ph) and $P(OMe)_3$. The synthesis of [(exo-5-dimethylphosphino-exo-6-R-η^5-cyclohexadiene)$Mn(CO)_2NO$] (R = Me, Ph, and $CH_2C(O)CH_3$), **7**, has been the subject of a preliminary communication[6].

Experimental

Elemental analyses were performed by Yanaco, MT-2 Elemental Analyzer at the chemical Analytic Center of the College of Engineering, Seoul National University. ^1H and ^{13}C-NMR spectra were measured on either Bruker AC 80 or Varian XL-200. Infrared spectra were recorded on a Perkin-Elmer 782 spectrometer and mass spectra were recorded on a VG ZAB-E double focusing mass spectrometer.

All solvents were purified by standard methods and all synthetic procedures were done under a nitrogen atmosphere. The [(arene)$Mn(CO)_3$]PF_6, [(cyclohexadienyl)$Mn(CO)_3$], and [(cyclohexadienyl)$Mn(CO)_2NO$]PF_6 were synthesized as previously described[7].

Preparation of 3. A 2 mole excess of PPh_3 was added to the corresponding compound in CH_2Cl_2. After stirring for 1 hr, an excess of diethyl ether was added to the reaction mixture to precipitate the product. The precipitate was filtered and washed several times with diethyl ether. The yield was 90% (R = Ph). R = Me: IR ν(CO and NO) 2040, 1778 cm^{-1}. R = Ph: IR ν(CO and NO) 2044, 1784 cm^{-1}. ^1H NMR ($CDCl_3$) δ 6.47 (d, J = 5 Hz, H^3), 4.83 (m, H^4), 3.86 (m, H^6), 3.52 and 3.11 (m, H^1 and H^5), 3.74 (s, OMe), 7.2-7.6 (m, Ph). Anal. Calcd for $C_{32}H_{28}F_6MnNO_3P_2$: C, 54.48; H, 4.00; N, 1.99. Found: C, 55.11; H, 3.79; N, 1.79.

Preparation of 4. A 1.5 mole excess of $MePPh_2$ was added to the suspension of the corresponding compound in CH_2Cl_2 at −20 °C. After stirring for 1 hr, an excess of diethyl ether was added to precipitate the unreacted salt and the CO-displaced one. After removal of the precipitates, the filtrate was concentrated and column chromatographed on basic alumina with diethyl ether, and then with CH_2Cl_2. The first coming out was $PMePh_2$ and the second one is the pro-